

High-pressure Raman spectroscopy study of wurtzite ZnO

Fredéric Decremps, Julio Pellicer-Porres,* A. Marco Saitta, Jean-Claude Chervin, and Alain Polian
*Physique des Milieux Condensés, CNRS-UMR 7602, Université Pierre & Marie Curie, B77, 4, place Jussieu,
 75252 Paris CEDEX 05, France*

(Received 10 July 2001; revised manuscript received 25 October 2001; published 6 February 2002)

The high-pressure behavior of optical phonons in wurtzite zinc oxide (*w*-ZnO) is studied using room-temperature Raman spectroscopy and *ab initio* calculations based on a plane-wave pseudopotential method within the density-functional theory. The pressure dependence of the zone-center phonons (E_2 , A_1 , and E_1) was measured for the wurtzite structure up to the hexagonal→cubic transition near 9 GPa. Above this pressure no active mode was observed. The only negative Grüneisen parameter is that of the E_2^{low} mode. E_1 (LO) and (TO) frequencies increase with increasing pressure. The corresponding perpendicular tensor component of the Born's transverse dynamic charge e_T^* is experimentally found to increase under compression like $e_T^*(P) = 2.02 + 6.4 \times 10^{-3}P$, whereas calculations give $e_T^*(P) = 2.09 - 2.5 \times 10^{-3}P$ (in units of the elementary charge e , P in GPa). In both cases, the pressure variation is small, indicating a weak dependence of the bond ionicity with pressure. The pressure dependence of the optical mode energies is also compared with the prediction of a model that treats the wurtzite-to-rocksalt transition as an homogeneous shear strain. There is no evidence of an anomaly in the E_2 and A_1 mode behaviors before the phase transition.

DOI: 10.1103/PhysRevB.65.092101

PACS number(s): 64.70.Dv, 78.30.-j, 91.60.Gf

Zinc oxide belongs to the wide-band-gap semiconductor family, with large ionic characters of chemical bonds.¹ The ionic size or relative electronegativity has been used to explain high pressure structure changes in $A^N B^{8-N}$ semiconductors. First-principles calculations have shown that the zinc-blende (or wurtzite)→rocksalt→ β -Sn transition sequence is a common feature for most semiconductors. However, a recent experimental identification of intermediate phases (like cinnabar in CdTe for example) and the systematic absence of some phases [rocksalt (*rs*) for covalent compounds and β -Sn for all except the most covalent] invalidate the traditional transition sequence and, consequently, question the standard theoretical approach. In a recent paper, Ozoliņš and Zunger² suggested that phase transitions are accompanied by phonon softening, whose instability has to be taken into account in the calculation to correctly predict the phase diagram. The latter outcome can also be discussed in terms of the transition mechanism, where the presence of negative Grüneisen parameters of phonon modes may play an important role. Recently, an intermediate structure was proposed in the wurtzite to rocksalt transformation path of GaN, along which the optical A_1 and E_2^{high} modes are expected to be affected by the bond formations.³ Wurtzite ZnO, which transforms under pressure into the *RS* phase at 9 GPa, may provide a good example of this trend.

Wurtzite ZnO belongs to the C_{6v}^4 ($P6_3mc$) space group. The primitive cell includes two formula units, with all atoms occupying $2b$ sites of symmetry C_{3v} . At the Γ point of the Brillouin zone, group theory predicts the existence of the following optic modes: $\Gamma_{opt} = A_1 + 2B_1 + E_1 + 2E_2$. The frequency from the B_1^{low} and B_1^{high} silent modes has been calculated at 260 and 540 cm^{-1} respectively. A_1 , E_1 , and E_2 modes are Raman active. In addition, A_1 and E_1 are infrared active, and therefore split into longitudinal and transverse optical (LO and TO) components. The mode assignment at ambient conditions is well established in the literature.⁴ To

the best of our knowledge, no calculation and only two experimental attempts have been made to study the *w*-ZnO phonon frequency shift under pressure.^{5,6} In the first reference, the authors reported the evolution of two phonon frequencies E_2^{high} and E_2^{low} over a relative small pressure range (0–1 GPa). In the second reference, the pressure dependence of four Raman modes [E_2^{high} , E_2^{low} , A_1 (TO), and E_1 (TO)] are given up to ~ 7.5 GPa. However no experimental details is described, neither on the sample nor on the apparatus (high-pressure cell, pressure-transmitting medium, or pressure measurement). This lack of information is detrimental to any discussion, especially in our case where, on compression at room temperature, non hydrostatic stresses are known to affect the phonon response of the crystal considerably. Here we report results on the high-pressure behavior of optical phonons in *w*-ZnO from both Raman experiments and *ab initio* calculations.

For the high-pressure Raman experiments, two samples were cut as platelets from a large, colorless, and transparent single-crystalline cube of *w*-ZnO purchased from SPC Goodwill. The sample was tailored to have a $30 \times 20 \mu\text{m}^2$ surface and to be 20 μm thick. One crystal was polished with plane parallel surfaces normal to the hexagonal c axis, and the other one with surfaces normal to the a axis. The high pressure cell was a membrane diamond-anvil cell (DAC).⁷ A stainless-steel gasket was preindented to 50 μm , and a 200 μm hole was drilled in the center by spark erosion. Neon gas loaded at high pressure (0.15 GPa) was used as a pressure-transmitting medium because (i) it is hydrostatic up to 16 GPa,⁸ (ii) it is chemically inert, and (iii) it has no luminescence and no Raman activity. Pressure was systematically measured before and after each Raman spectra using the fluorescence emission of a ruby sphere⁹ placed close to the sample into the gasket hole. The accuracy was better than 0.1 GPa at the maximum pressure reached. Raman spectra were excited with the 514.5 nm line of an Ar^+ laser focused

TABLE I. Experimental and theoretical Raman-active w -ZnO Γ -point phonon frequencies (in cm^{-1}) at ambient conditions.

Mode	This work (exp.)	This work (theo.)	Ref. 13	Ref. 4
E_2^{low}	99	92	101	101
E_2^{high}	439	449	444	437
$A_1(\text{TO})$	382	397	380	380
$E_1(\text{TO})$	414	426	413	408
$A_1(\text{LO})$	574	559	579	574
$E_1(\text{LO})$	580	577	591	584

down to 5 μm with a power level of about 500 mW at the entrance of the DAC. The scattered light was analyzed with a Dilor XY triple spectrometer and a liquid-nitrogen-cooled CCD multichannel detector. All spectra were recorded in the backscattering geometry with unpolarized light. In this geometry, E_2 , $A_1(\text{TO})$, and $E_1(\text{TO})$ are allowed with incident radiation perpendicular to the c axis, and E_2 and $A_1(\text{LO})$ with light parallel to the c -axis. The Raman frequencies were determined from a computer fit of the peaks with a Lorentzian profile. The accuracy was better than 1 cm^{-1} .

Phonon frequencies, Born effective charges, and the dielectric constant ϵ_∞ were calculated from first-principles in the framework of density-functional theory and local-density approximation, by using the PWSCF code.¹⁰ We adopted the density-functional perturbation theory (DFPT) approach¹¹ and a standard local-density approximation plane-wave/pseudopotential scheme. Norm-conserving pseudopotentials of the Troullier-Martins form¹² have been used, with the inclusion of $3d$ electrons of Zn in the valence shell. Tests carried out with zinc $3d$ electrons in the core and nonlinear core correction gave an unsatisfactory accuracy of phonon frequencies. We used a cutoff of 70 Ry and a $8 \times 8 \times 4$ mesh of special k points for the Brillouin-zone integration. At each pressure, w -ZnO is relaxed with respect to the c/a ratio and the internal parameter u , and phonon frequencies are calculated at these optimized structural parameters. Because of the polar character of ZnO, the dynamical matrix displays a nonanalytical behavior in the limit $\mathbf{q} \rightarrow 0$, arising from the long-range character of the Coulomb forces. The calculations of LO modes is nonetheless straightforward, since the LO-TO splitting only depends on the phonon frequencies, the dielectric constant, and the Born effective charges, which can all be directly calculated in the DFPT framework.

Before performing the high-pressure experiment we examined the optical zone-center phonons of w -ZnO at ambient pressure, with light parallel and perpendicular to the c axis. We employed the large single crystal from which the micrometric samples used in the high-pressure experiments were extracted. The E_2 , $A_1(\text{TO})$, and $E_1(\text{TO})$ modes are clearly seen in the spectra. Conversely the $A_1(\text{LO})$ mode is hardly observable and not seen at high pressure (crystal in the DAC). The frequency assignment, as well as a comparison with *ab initio* results and previous works, is presented in Table I. The Raman spectra in both configurations also show additional features at 331 and 552 cm^{-1} . In Ref. 4 they

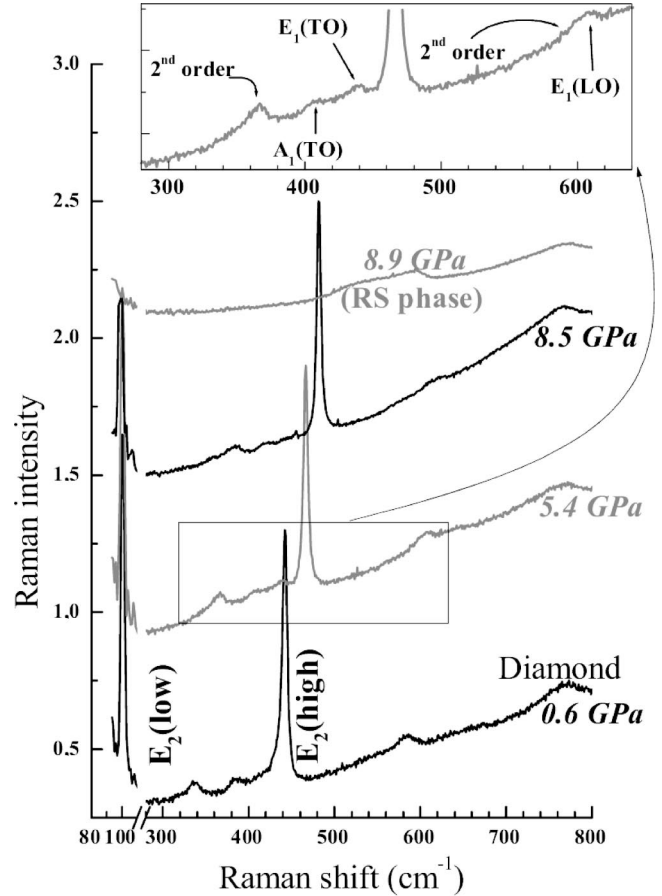


FIG. 1. Raman spectra of single-crystalline ZnO under different hydrostatic pressures in the backscattering geometry. The spectra are shifted upward for clarity.

were tentatively assigned to second-order structures by comparison with flat regions in the dispersion curves.

Under pressure, with incidence parallel to the c axis, only an E_2 single phonon mode was apparent when focusing at the center of the sample. In the same configuration, $A_1(\text{TO})$, $E_1(\text{TO})$ and a mode at 580 cm^{-1} appear, with the laser light focused on the sample border. This mode is much more intense than the $A_1(\text{LO})$ found in ambient conditions. Its frequency is also slightly higher. The $E_1(\text{LO})$ mode is forbidden in the backscattering geometry. However, it was observed in ZnO in the forbidden $X(\text{ZZ})\bar{X}$ geometry.⁴ We have thus assigned the mode appearing at 580 cm^{-1} to the $E_1(\text{LO})$ mode. Our assignment should be considered as tentative since this mode is observed only when we focus on the sample border. In this situation, the incidence direction with respect to the crystal axes is not defined, and mixed modes may be obtained. In this geometry, typical Raman spectra of ZnO at various pressures are shown in Fig. 1.

The pressure dependences of the phonon frequencies for the two high-pressure runs are shown in Fig. 2. No difference between the two runs is observed. Around 8.7 GPa, the disappearance of all Raman peaks reflects the onset of the wurtzite-rocksalt structural transformation in excellent agreement with the previous high-pressure studies. E_2^{low} is the only mode which exhibit a negative pressure dependence.

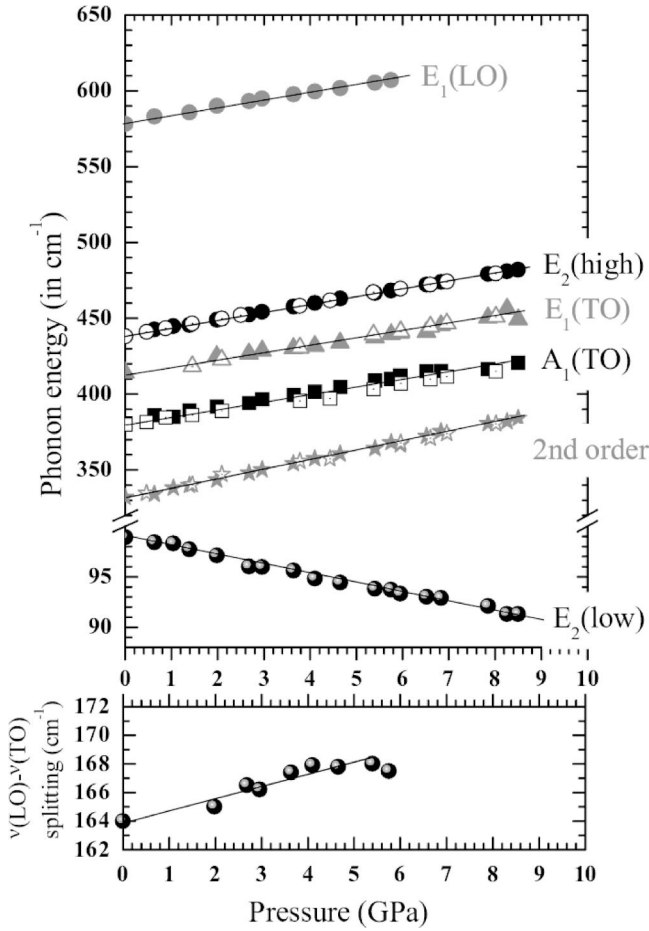


FIG. 2. Top: Pressure dependence of the observed optical phonons. Open (full) symbols: propagation of light perpendicular (parallel) to c . Bottom: $(\nu_{LO} - \nu_{TO})$ E_1 phonon mode splitting vs pressure. Solid lines are linear least-square fits to the experimental points.

The frequency shift of E_2^{high} , $A_1(\text{TO})$, $E_1(\text{TO})$, and $E_1(\text{LO})$ modes increase with pressure, and no anomaly up to the transition pressure is detected. The frequency dependence of E_2^{low} and E_2^{high} are in perfect agreement with the low-pressure values obtained from Mitra *et al.*⁵ On the other hand, while our frequency data seem to agree with those of Minomura⁶ [except $A_1(\text{TO})$], the discrepancy in the corresponding Grüneisen parameters is important [except for $E_1(\text{TO})$]; see Table II]. It is difficult to account for this dis-

TABLE II. ZnO mode Grüneisen parameters γ_i of the zone-center phonons

Symmetry	This work (expt.)	This work (theo.)	Ref. 6
E_2^{low}	-1.6	-1.67	-1.75
E_2^{high}	2.0	1.84	1.62
$A_1(\text{TO})$	2.1	1.70	1.70
$E_1(\text{TO})$	1.8	1.80	1.76
$E_1(\text{LO})$	1.4	1.30	-

agreement, since no calculation details was given in Ref. 6. We suspect that the author used a different bulk modulus. Here the mode Grüneisen parameters γ_i are defined as: $\gamma_i = -(d \ln \nu_i / d \ln V)_{P=0} = (B_0 d \nu_i / \nu_i dP)$. The isothermal Birch-Murnaghan equation of state was used to determine $B_0 = 170$ GPa and $B' = 4$ from the x-ray-diffraction data $V(P)$.¹⁴

The experimental LO-TO splitting of the E_1 phonon mode increases with a small pressure dependence (+2% at 5 GPa, see Fig. 2), in good agreement with theoretical results where no variation of the E_1 or A_1 LO-TO splitting is obtained in the same pressure range. It is noteworthy that this splitting increases (nearly constant from calculations) with pressure, an uncommon behavior for $A^N B^{8-N}$ semiconductors except SiC,¹⁵ AlN, and GaN.¹⁶ The change of the Born transverse dynamic charge e_T^* under compression can be determined from the measured frequencies using (in S.I. units) $(e_T^*)^2 = 4\pi^2 V \mu \epsilon_0 \epsilon_\infty (\nu_{LO}^2 - \nu_{TO}^2)$, where V is the volume per formula, μ is the reduced mass, ϵ_0 is the vacuum permittivity, and ϵ_∞ is the high frequency (optical) dielectric constant.¹⁷ At ambient pressure, and with $\epsilon_\infty(P=0) = 3.95\epsilon_0$, the experimental effective charge values are 2.02 and 2.4 (in units of the elementary charge e) for the E_1 and A_1 modes respectively. The evolution of the high-frequency dielectric constant ϵ_∞ under high pressure has not been measured. To our knowledge only the dependences of the ordinary (n_o) and extraordinary (n_e) refractive indices at $0.5893 \mu\text{m}$ were measured.¹⁸ In order to estimate the pressure behavior of e_T^* from our measurements, we suppose that the pressure dependences of ϵ_∞ and n_o^2 are equal. With this assumption, we obtain (in S.I. units) $(\partial \epsilon_\infty / \partial P)_{P=0} = 2n_o(\partial n_o / \partial P)_{P=0} = -0.014\epsilon_0 \text{ GPa}^{-1}$. The behavior under pressure of the normalized perpendicular tensor component $e_T^*/e_T^*(0)$ is plotted in Fig. 3. The effective charge in w -ZnO increases under compression with $\partial e_T^* / \partial P = 6.4 \times 10^{-3}$ (in units of the elementary charge e per GPa). Theoretically, ϵ_∞ and the effective charge have been found to decrease linearly with pressure: $(\partial \epsilon_\infty / \partial P)_{P=0} = -0.025\epsilon_0 \text{ GPa}^{-1}$ and $\partial e_T^* / \partial P = -2.5 \times 10^{-3}$. However, if we constrain the calculations to use the experimental pressure dependence of ϵ_∞ , we obtain $\partial e_T^* / \partial P = 0$. These results may indicate a small variation of the w -ZnO bond ionicity when compressed between 0 and 4 GPa. In comparison, the $\partial e_T^* / \partial P$ experimental value for SiC (Ref. 15) is 5.3×10^{-3} , 0.15×10^{-3} for AlN,¹⁶ and -1.3×10^{-3} for GaN.¹⁶ Above 4 GPa, Fig. 3 shows a saturation of e_T^* . However, the refractive indices (and thus the dielectric constant) have only been measured between 0 and ~ 1 GPa,¹⁸ which means that our $e_T^*(P)$ values above that pressure range have been obtained from an extrapolation of $\epsilon_\infty(P)$.

We now turn the discussion to the simple homogeneous orthorhombic shear strain path proposed to picture the w to rs mechanism of transition.³ This model predicts that, under pressure, a relaxation of the structural parameter u from $\sim \frac{3}{8}$ up to $\frac{1}{2}$ is expected to occur in the wurtzite structure (i.e., below the phase transition) which gives rise to a new

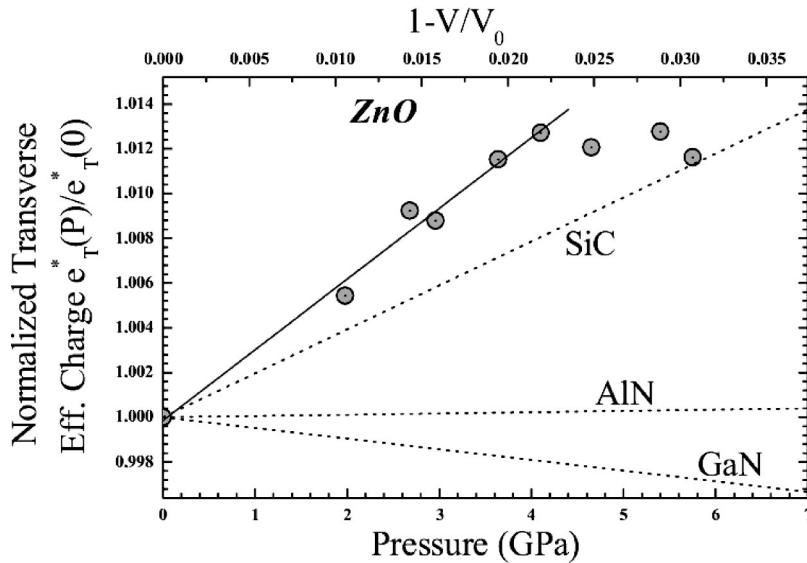


FIG. 3. Experimental pressure and volume dependence of the perpendicular component e_T^* under compression normalized to its ambient pressure value $e_T^*(0) = 2.02$. For comparison, dotted lines represent the experimental values of e_T^* for SiC (Ref. 15), AlN (Ref. 16), and GaN (Ref. 16).

intermediate phase isomorphic to h -MgO. In addition to the expected (and experimentally observed) negative mode Grüneisen parameter of $E_{2^{low}}^2$ at Γ , the previous model predicts the optic A_1 and E_2^{high} modes at Γ to be affected by the $w \rightarrow h$ -MgO transition. However, in the pressure range probed during the present work (from atmospheric up to the transition pressure, i.e., 9 GPa), no instability of these modes is observed. Our results show a discrepancy with the A_1 and E_1 anomaly expected from calculations, and agree with the conclusions derived from long-range order probe (x-ray-diffraction experiments) by Desgreniers,¹⁹ where the evaluation of the normalized integrated intensity of the (002) and (101) diffraction lines indicated no deviation of the u parameter from its ideal value.

In summary, the LO-TO splitting of the E_1 phonon mode has been experimentally and theoretically found to be weakly pressure dependent. This unusual behavior is related to a small variation of the chemical bonds ionicity of w -ZnO with pressure. Moreover, the present observation of an optical phonon under pressure does not show any softening of the optic A_1 and E_2^{high} modes as theoretically expected.³ All

Grüneisen parameters show positive values except that of E_2^{low} , which is a quite common feature in II-VI compounds. However, from first-principles calculation on w -ZnO, we predict (in good agreement with Ref. 3) the u parameter to shift up to 0.5 at a volume of 24.08 \AA^3 (i.e., ~ 21 GPa). Experimentally, the w -to- rs first-order transition limits the pressure range of w structure existence and, consequently, does not allow the second-order process observation (via optical-phonons instabilities for example). However, if we refer to the phase diagram of ZnO,²⁰ it may be possible to constrain the structure to still be tetrahedrally coordinated at low temperature in order to cause the wurtzite \rightarrow NaCl transition to occur at higher pressure, rendering the second-order process directly observable in semiconductors.

We wish to acknowledge Bernard Couzinet for the neon DAC loading. One of us (A.M.S.) acknowledges the Institut du Développement et des Ressources en Informatique Scientifique (IDRIS) for computer time allocation (Project No. 11387-CP9). This research was partly supported by a Marie Curie fellowship of the European Community, No. HPMF CT2000-00764.

*Permanent address: Institut de Ciència dels Materials, Universitat de València, Departamento de Física Aplicada, Edifici Investigació, E-46100 Burjassot (València), Spain.

¹A. Garcia and M.L. Cohen, Phys. Rev. B **47**, 4215 (1993).

²V. Ozoliņš and A. Zunger, Phys. Rev. Lett. **82**, 767 (1999).

³S. Limpijumngong and W.R.L. Lambrecht, Phys. Rev. Lett. **86**, 91 (2001); J. Serrano *et al.*, Phys. Rev. B **62**, 16 612 (2000).

⁴J.M. Calleja and M. Cardona, Phys. Rev. B **16**, 3753 (1977).

⁵S.S. Mitra *et al.*, Phys. Rev. **186**, 942 (1969).

⁶S. Minomura, *High Pressure in Science and Technology, Proceedings of the 9th AIRAPT International High Pressure Conference* (Elsevier, New York, 1984), p. 277.

⁷R. Letoullec *et al.*, High Press. Res. **1**, 77 (1988).

⁸H.K. Mao *et al.*, J. Geophys. Res. B **91**, 4673 (1986).

⁹G.J. Piermarini *et al.*, J. Appl. Phys. **46**, 2774 (1975).

¹⁰PWSCF code: www.pwscf.org

¹¹S. Baroni *et al.*, Phys. Rev. Lett. **58**, 1861 (1987); P. Giannozzi *et al.*, Phys. Rev. B **43**, 7231 (1991).

¹²N. Troullier and J.M. Martins, Phys. Rev. B **43**, 1993 (1991).

¹³C.A. Arguello *et al.*, Phys. Rev. **181**, 1351 (1969).

¹⁴F. Decremps *et al.* (unpublished).

¹⁵J. Liu and Y.K. Vohra, Phys. Rev. Lett. **72**, 4105 (1994); K. Karch and F. Bechstedt, *ibid.* **77**, 1660 (1996).

¹⁶A.R. Goñi *et al.*, Phys. Rev. B **64**, 035205 (2001).

¹⁷M. Born and K. Huang, *Dynamical Theory of Crystal Lattices* (Clarendon, Oxford, 1954), Chap. 2.

¹⁸K. Vedam and T.A. Davis, Phys. Rev. **181**, 1196 (1969).

¹⁹S. Desgreniers, Phys. Rev. B **58**, 14 102 (1998).

²⁰F. Decremps *et al.*, Europhys. Lett. **51**, 268 (2000).